Nano Today (2010) **5**, 540—552

available at www.sciencedirect.com

ScienceDirect

journal homepage: www.elsevier.com/locate/nanotoday

REVIEW

Piezopotential gated nanowire devices: Piezotronics and piezo-phototronics

Zhong Lin Wang*

School of Material Science and Engineering, Georgia Institute of Technology, Atlanta, GA 30332-0245, USA

Received 11 October 2010; received in revised form 25 October 2010; accepted 28 October 2010

KEYWORDS
ZnO;
Nanowire;
Piezopotential;
Piezotronics;
Piezo-phototronics

Summary Due to the polarization of ions in a crystal that has non-central symmetry, a piezoelectric potential (*piezopotential*) is created in the crystal by applying a stress. For materials such as ZnO, GaN, and InN in the wurtzite structure family, the effect of piezopotential on the transport behavior of charge carriers is significant due to their multiple functionalities of piezoelectricity, semiconductor and photon excitation. By utilizing the advantages offered by these properties, a few new fields have been created. Electronics fabricated by using inner-crystal piezopotential as a ''gate'' voltage to tune/control the charge transport behavior is named *piezotronics*, with applications in strain/force/pressure triggered/controlled electronic devices, sensors and logic units. *Piezo-phototronic effect* is a result of three-way coupling among piezoelectricity, photonic excitation and semiconductor transport, which allows tuning and controlling of electro-optical processes by strain induced piezopotential. The objective of this review article is to introduce the fundamentals of piezotronics and piezo-phototronics and to give an updated progress about their applications in energy science and sensors.

Piezoelectricity, a phenomenon known for centuries, is an effect that is about the production of electrical potential in a substance as the pressure on it changes. The most well known material that has piezoelectric effect is the provskite structured Pb(Zr, Ti)O_3 (PZT), which has found huge applications in electromechanical sensors, actuators and energy generators. But PZT is an electric insulator and it is less useful for building electronic devices. Piezoelectricity has its own field and is being largely studied in the ceramic community. Wurtzite structures, such as ZnO, GaN, InN and ZnS, also have piezoelectric properties but they are not extensively used as much as PZT in piezoelectric sensors and actuators due to their small piezoelectric coefficient. Therefore, the study of wurtzite structures is mainly in the electronic and photonic communities due their semiconductor and photon excitation properties.

In this review, we will explore the piezopotential [1—4] generated in the wurtzite structures and how to use it to serve as a ''gate'' voltage for fabricating new electronics [5,6]. One of the most common electronic devices is a single channel field effect transistor (FET) based on a semiconductor nanowire (NW), in which a source and drain are located at the two ends of the device, and a gate voltage is applied to the channel and the substrate [7,8]. By applying a source to drain driving voltage, V_{DS}, the charge carrier trans-

* Corresponding author.
E-mail addresses: zhong.wang@mse.gatech.edu, zlwang@gatech.edu

1748-0132/$ — see front matter © 2010 Elsevier Ltd. All rights reserved.
doi:10.1016/j.nantod.2010.10.008

port process in the semiconductor device is tuned/gated by the gate voltage V_G, which is an externally applied potential. Alternatively, the gate voltage can be replaced by the piezopotential generated inside the crystal (inner potential), so that the charge carrier transport process in FET can be tuned/gated by applying a stress to the device [9,10]. This type of device is called piezotronic device as triggered or driven by a mechanical deformation action. Alternatively, for a device with Schottky contacts at either or both of the source or drain, by introducing a laser excitation at the source/drain, a coupling has been demonstrated among piezoelectricity, photoexcitation and semiconductor characteristics, leading to the piezo-phototronic effect [11]. This paper is to review the principle and potential applications of the piezotronics and piezo-phototronics.

Piezoelectricity and piezopotential

We now use ZnO to elaborate the structure and piezopotential in wurtzite family. Wurtzite crystal has a hexagonal structure with a large anisotropic property in *c*-axis direction and perpendicular to the *c*-axis. The crystal lacks of center symmetry, which is the core of piezoelectricity due to the intrinsic crystallographic structure. Simply, the Zn^{2+} cations and O^{2-} anions are tetrahedrally coordinated and the centers of the positive ions and negatives ions overlap with each other. Therefore, the crystal shows no polarization under strain-free condition. If a stress is applied at an apex of the tetrahedron, the center of the cations and the center of anions are relatively displaced, resulting in a dipole moment (Fig. 1A). A constructive adds up of the dipole moments created by all of the units in the crystal results in a macroscopic potential drop along the straining direction in the crystal. This is the piezoelectric potential (*piezopotential*) (Fig. 1B) [5,6]. The piezopotential, an inner potential in the crystal, is created by the non-mobile, non-annihilative ionic charges, the piezopotential remains in the crystal as long as the stress remains. The magnitude of the piezopotential depends on the density of doping and the strain applied.

The distribution of piezopotential in a ZnO NW has been calculated using the Lippman theory [12,13]. For simplicity, we first ignore doping in ZnO so that it is assumed to be an insulator. For a one-end fixed free-standing NW that is transversely pushed by an external force, the stretched side and the compressed side surfaces exhibit positive and negative piezopotential (Fig. 1B), respectively, which can act as a transverse voltage for gating the charge transport along the NW [1]. An alternative geometry is a simple two-end bonded single wire with a length of 1200 nm and a hexagonal side length of 100 nm [8]. When a stretching force of 85 nN is uniformly acting on the NW surfaces surrounded by electrodes in the direction parallel to *c*-axis, it creates a potential drop of approximately 0.4 V between the two end sides of the NW with the $+c$ axis side of higher potential. When the applied force changes to a compressive, the piezoelectric potential reverses with the potential difference remaining 0.4 V but with the $-c$ axis side at a higher potential.

The presence of the piezopotential in the crystal has created a few new research fields. A nanogenerator has

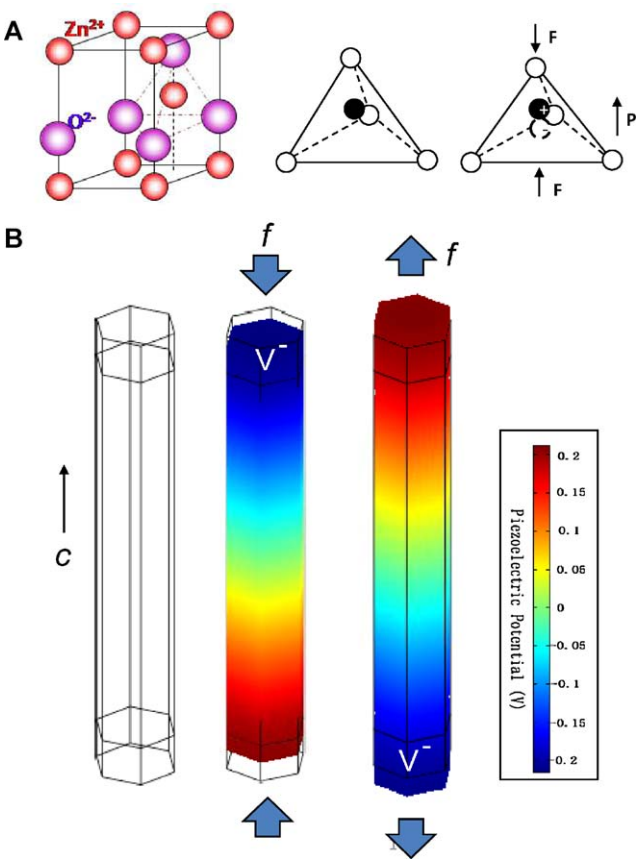

Figure 1 Piezopotential in wurtzite crystal. (A) Atomic model of the wurtzite-structured ZnO. (B) Numerical calculation of the piezoelectric potential distribution in a ZnO nanowire under axial strain. The growth direction of the nanowire is *c*-axis. The dimensions of the nanowire are $L = 600$ nm and $a = 25$ nm; the external force is $f_y = 80$ nN.
From [13].

been developed for converting mechanical energy into electricity [1,14—17]. Once a strained piezoelectric crystal is connected at its two polar ends to an external electric load, the piezopotential creates a drop in the Fermi levels at the two contact ends, thus, the free electrons in the external load are driven to flow from one side to the other to ''screen'' the local piezopotential and reach a new equilibrium. The generated current in the load is a result of the transient flow of electrons. An alternating flow of electrons is possible if the piezopotential is continuously changed by applying a dynamic stress across the crystal. This means that the nanogenerator gives continuous output power if the applied stress is varying, which means inputting mechanical work. The nanogenerator has been extensively developed and it is now gives an output of $\sim$3 V, and the output power is able to drive a liquid crystal display (LCD), light emitting diode and laser diode [18—21]. The nanogenerator will play an important role in energy harvesting as the sustainable and self-sufficient power sources for the micro/nano-systems. We now introduce the electronic processes induced by the piezopotential in the next few sections.

Piezopotential gated electronic and photonic processes

Piezotronic and piezophotonic effects [6]

A most simple FET is a two end bonded semiconductor wire, in which the two electric contacts at the ends are the source and drain, and the gate voltage can be applied either at the top of the wire through a gate electrode or at its bottom on the substrate. When a ZnO NW is strained axially along its length, two typical effects are observed. One is the *piezoresistance effect*, which is introduced because of the change in bandgap and possibly density of states in the conduction band. This effect has no polarity so that it has equivalent/identical effect on the source and drain of the FET. On the other hand, piezopotential is created along its length. For an axial strained NW, the piezoelectric potential continuously drops from one side of the NW to the other, which means that the electron energy continuously increases from one side to the other. Meanwhile, the Fermi level will be flat all over the NW when equilibrium is achieved, since there is no external electrical field. As a result, the effective barrier height and/or width of the electron energy barrier between ZnO and metal electrode will be raised at one side and lowered at the other side, thus, it has a non-symmetric effect on the source and drain. This is the *piezotronic effect* [5].

A better understanding about the piezotronic effect is to compare it with the most fundamental structure in semiconductor devices: Schottky contact and p—n junction. When a metal and a n-type semiconductor forms a contact, a Schottky barrier (SB) ($e\phi_{SB}$) is created at the interface if the work function of the metal is appreciably larger than the electron affinity of the semiconductor (Fig. 2A). Current can only pass through this barrier if the applied external voltage is larger than a threshold value (ϕ_i) and its polarity is with the metal side positive (for n-type semiconductor). If a photon excitation is introduced, the newly generated electron—hole pairs not only largely increase the local conductance, but also reduce the effective height of the SB as a result of charge redistribution (Fig. 2B).

Once a strain is created in the semiconductor that also has piezoelectric property, a negative piezopotential at the semiconductor side effectively increases the local SB height to $e\phi'$ (Fig. 2C), while a positive piezopotential reduces the barrier height. The polarity of the piezopotential is dictated by the direction of the *c*-axis for ZnO. The role played by the piezopotential is to effectively change the local contact characteristics through an internal field, thus, the charge carrier transport process is tuned/gated at the metal—semiconductor (M—S) contact. By considering the change in piezopotential polarity by switching the strain from tensile to compressive, the local contact characteristics can be tuned and controlled by the magnitude of the strain and the sign of strain. This is the core of piezotronics.

When a p-type and a n-type semiconductors form a junction, the holes in the p-type side and the electrons in the n-type side tend to redistribute to balance the local potential, the interdiffusion and recombination of the electrons and holes in the junction region forms a charge depletion zone (Fig. 3A). Once an external potential is applied across the junction with the n-type side positive, the width of the charge depletion zone is enlarged, thus, few charge carriers flow across it. But once the p-type side is applied with a positive bias and when the strength of the bias is high enough to overcome the barrier formed by the depletion zone, charge carrier can flow across the junction. This is the working principle of the pn diode.

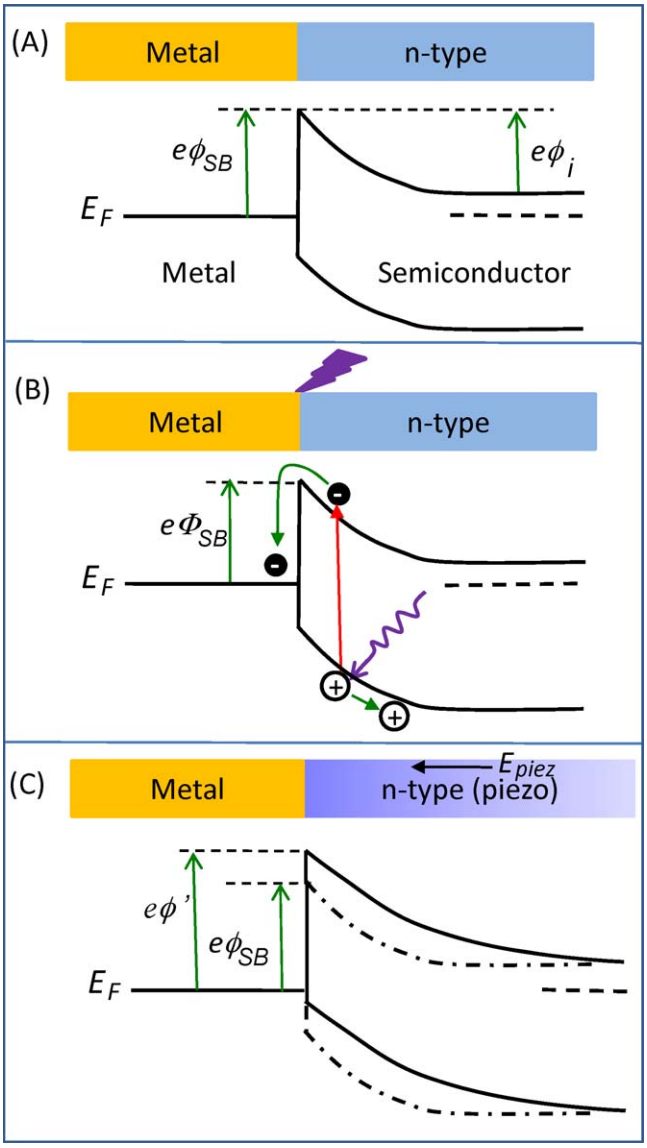

Figure 2 Energy band diagram for illustrating the effects of laser excitation and piezoelectricity on a Schottky contacted metal—semiconductor interface. (A) Band diagram at a Schottky contacted metal—semiconductor interface. (B) Band diagram at a Schottky contact after exciting by a laser that has a photon energy higher than the bandgap, which is equivalent to a reduction in the Schottky barrier height. (C) Band diagram at the Schottky contact after applying a strain in the semiconductor. The piezopotential created in the semiconductor has a polarity with the end in contacting with the metal being low.

With the creation of a piezopotential in one side of the semiconductor material under strain, the local band structure near the pn junction is changed/modified. For easy understanding, we include the screening effect of the charge carriers to the piezopotential in the discussion, which

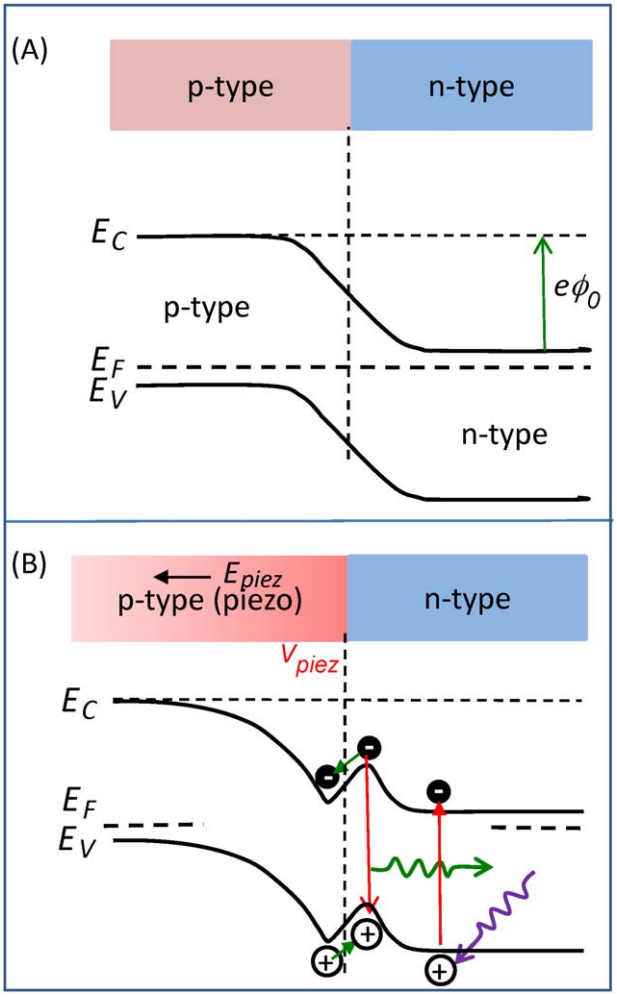

Figure 3 Energy band diagram for illustrating the effect of piezoelectricity on a pn junction. (A) Band diagram at a conventional pn junction made by two semiconductors have almost the same bandgaps. (B) Band diagram of the pn junction with the presence of a piezopotential at the p-type side with a polarity of higher potential at the junction side (see text).

means that the positive piezopotential side in n-type material is largely screened by the electrons, while the negative piezopotential side is almost unaffected. By the same token, the negative piezopotential side in p-type material is largely screened by the holes, but leaves the positive piezopotential side almost unaffected. As shown in Fig. 3B for a case that the p-type side is piezoelectric and a strain is applied, the local band structure is largely changed, which significantly affects the characteristic of charge carriers flow through the interface. This is the core of the piezotronic effect. In addition, the holes in the p-type side can drift to the n-type side to combine with the electrons in the conduction band, possibly resulting in an emission of photon. This is a process of piezopotential induced photon emission, e.g., *piezophotonics* [2]. The following conditions may need to be met in order to observe the piezophotonic process. The magnitude of the piezopotential has to be significantly large in comparison to ϕ_i, so that the local piezoelectric field is strong enough to drive the diffusion of the holes across the pn junction. The straining rate for creating the piezopotential has to be rather large, so that the charge carriers are driven across the interface within a time period shorter than the time required for charge recombination. The width of the depletion layer has to be small so that there are enough charge carriers available in the acting region of the piezopotential. Finally, a direct bandgap material is beneficial for the observation of the phenomenon.

The fundamental working principles of the p—n junction and the Schottky contact are that there is an effective barrier that separates the charge carriers at the two sides to across. The height and width of the barrier are the characteristic of the device. In piezotronics, the role played by the piezopotential is to effectively change the width of p—n junction or height of SB by piezoelectricity.

Piezo-phototronic effect

For a material that simultaneously has semiconductor, photon excitation and piezoelectric properties, besides the well known coupling of semiconductor with photon excitation process to form the field of optoelectronics, additional effects could be proposed by coupling semiconductor with piezoelectric to form a field of piezotronics, and piezoelectric with photon excitation to form a field of piezophotonics. Furthermore, a coupling among semiconductor, photon excitation and piezoelectric is a field of *piezo-phototronics* [11], which can be the basis for fabricating piezo-photonic—electronic nanodevices. The piezo-phototronic effect is about the tuning and controlling of electro-optical processes by strain induced piezopotential (Fig. 4). The applications of piezo-phototronics will be elaborated later.

Piezotronic devices and applications

Piezodiode

A simple piezotronic device is a polarity switchable diode that is made of a ZnO NW contacted with metal contacts at the two ends on an insulator polymer substrate [22,23]. From the initial *I—V* curve measured from the device before applying a strain as shown in Fig. 5A, the symmetric shape of the curve indicates that the SBs present at the two contacts are about equal heights. The equivalent circuit model of the device is a pair of back-to-back Schottky diodes, as illustrated in the inset in Fig. 5A. Under tensile strain, the piezoelectric potential at the right-hand side of this NW was lower (denoted by blue color in the inset in Fig. 5A), which raised the local barrier height (denoted by a large diode symbol in the inset). Since the positive piezoelectric potential was partially screened by free electrons, the SB height at the left-hand side remained almost unchanged. As a result, under positive bias voltage with the left-hand side positive, the current transport was determined by the reverse biased SB at the right-hand side. While under the reverse biased voltage with the right-hand side positive, the current transport depended on the reverse biased SB at the left-hand side, which had a much lower barrier height than the right-hand side one. Experimentally, the device thus exhibited a rectifying behavior in the positive voltage region, and the *I—V* curve in the negative voltage region overlapped with

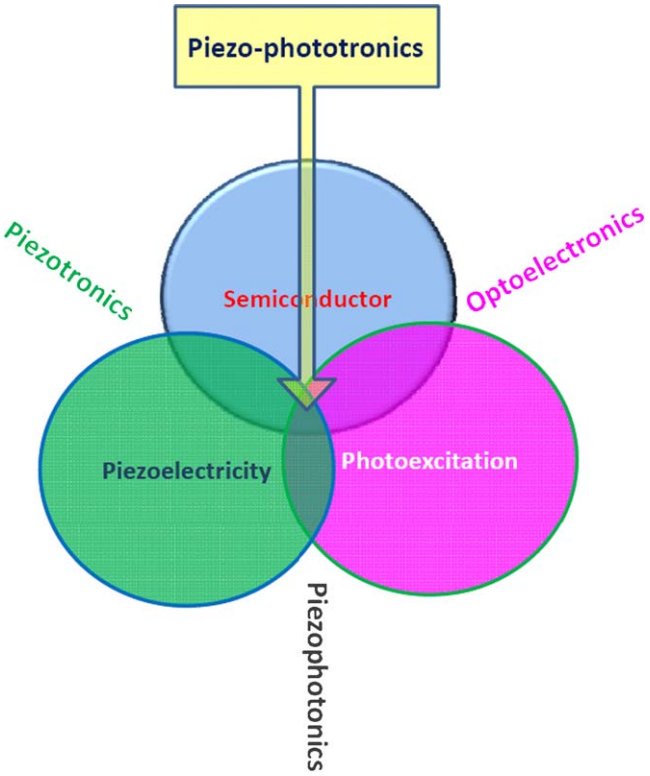

Figure 4 Schematic diagram showing the three-way coupling among piezoelectricity, photoexcitation and semiconductor, which is the basis of piezotronics (piezoelectricity—semiconductor coupling), piezophotonics (piezoelectric—photon excitation coupling), optoelectronics, and piezo-phototronics (piezoelectricity—semiconductor—photoexcitation). The core of these coupling relies on the piezopotential created by the piezoelectric materials.

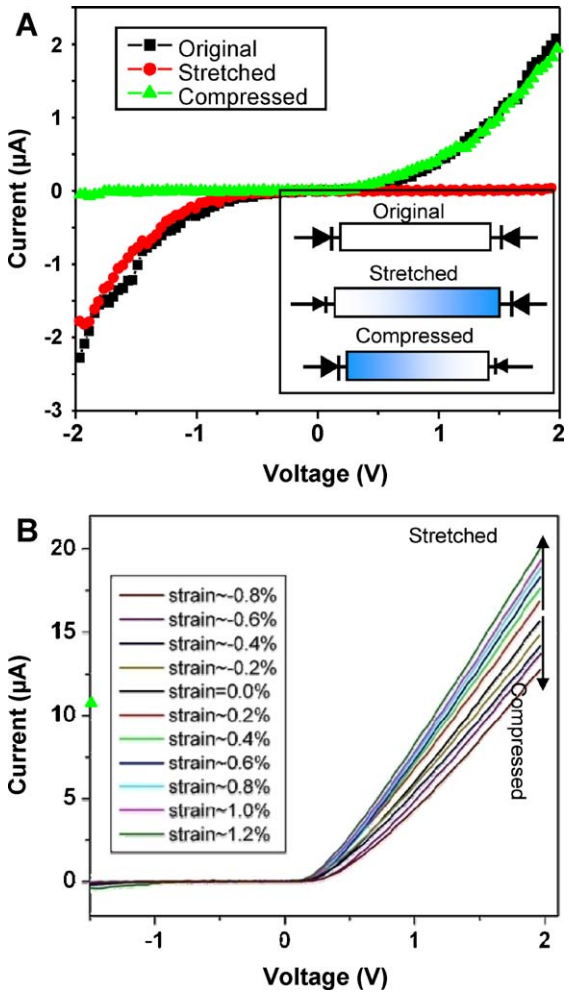

Figure 5 Piezotronic strain sensor/switch. (A) Changes of transport characteristics of an Ag/ZnO-nanowire/Ag device from symmetric I—V characteristic (black) to asymmetric rectifying behavior when stretching (red) and compressing (green) the wire. The inset is the equivalent circuit models of the device in corresponding to the observed I—V curves, different sizes of diode symbol are used to illustrate the asymmetric Schottky contacts at the two ends of the nanowire. The blue side is the negative potential side, and the other side is positive side. (B) I—V characteristic of an Ag/ZnO-nanowire/Ag device measured under different axial strains, showing its application as a strain sensor (For interpretation of the references to colour in this figure legend, the reader is referred to the web version of the article.)
From [22,23].

that of the original curve without straining. By the same token, under compressive strain the device exhibited a rectifying behavior in the negative voltage region, and the I—V curve in the positive voltage region overlapped with that of the original curve without straining, as shown by the green line in Fig. 5A. Studies by others groups also support the proposed model [24—28].

Piezotronic logic operations [29]

The existing semiconductor NW logic devices are based on electrically gated field effect transistors (FETs), which function as both the drivers and the active loads of the logic units by adjusting the conducting channel width [30]. Moreover, the currently existing logic units are ''static'' and are almost completely triggered or agitated by electric signals, while the ''dynamic'' movable mechanical actuation is carried out by another unit possibly made of different materials. It is highly desirable to integrate the static logic operations with the dynamic mechanical action into one unit utilizing a single material. We demonstrated the first piezoelectric trigged mechanical-electronic logic operation using the piezotronic effect, through which the integrated mechanical actuation and electronic logic computation are achieved using only ZnO NWs.

A strain gated transistor (SGT) is made of a single ZnO NW with its two ends, which are the source and drain electrodes, being fixed by silver paste on a polymer substrate (Fig. 6A) [29]. Once the substrate is bent, a tensile/compressive strain is created in the NW since the mechanical behavior of the entire structure is determined by the substrate. Utilizing the piezopotential created inside the NW, the gate input for a NW SGT is an externally applied strain rather than an electrical signal. $I_{DS} - V_{DS}$ characteristic for each single ZnO-NW SGT is obtained as a function of the strain created in the SGT (Fig. 6A) before further assembly into logic

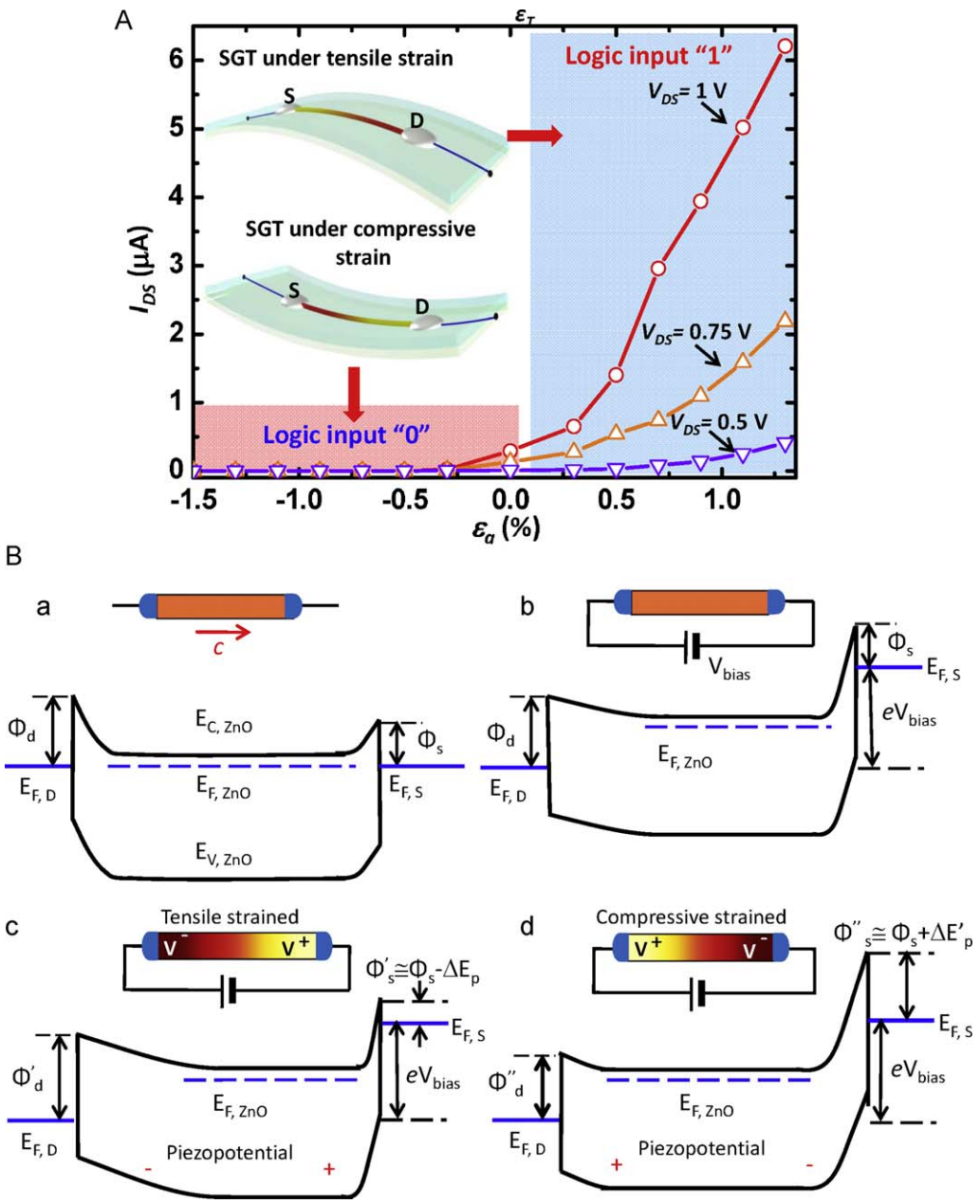

Figure 6 Strain-gated transistor (SGT). (A) Current—strain (I_{DS}—ε_g) transfer characteristic for a ZnO SGT device with strain sweeping from $\varepsilon_g = -0.53\%$ to 1.31% at a step of 0.2%, where the V_{DS} bias values were 1 V, 0.75 V and 0.5 V, respectively. (B) The band structures of the ZnO NW SGT under different conditions for illustrating the mechanism of SGT. The crystallographic *c*-axis of the nanowire directs from drain to source. (a) The band structure of a strain-free ZnO NW SGT at equilibrium with different barrier heights of Φ_S and Φ_D at the source and drain electrodes, respectively. (b) The quasi-Fermi levels at the source ($E_{F,S}$) and drain ($E_{F,D}$) of the ZnO SGT are split by the applied bias voltage V_{bias}. (c) With tensile strain applied, the SBH at the source side is reduced from Φ_S to $\Phi'_S \cong \Phi_S - \Delta E_P$. (d) With compressive strain applied, the SBH at the source side is raised from Φ_S to $\Phi''_S \cong \Phi_S + \Delta E'_P$. From [29].

devices. A NW SGT is defined as forward biased if the applied bias is connected to the drain electrode (Fig. 6A). For a SGT, the external mechanical perturbation induced strain (ε_g) acts as the gate input for controlling the ''on''/''off'' state of the NW SGT. The positive/negative strain is created when the NW is stretched/compressed. The SGT behaves in a similar way to a *n*-channel enhancement-mode MOSFET, apparently indicating the working principle of the SGT.

The working principle of a SGT is illustrated by the band structure of the device [22,23]. A strain free ZnO NW may have Schottky contacts at the two ends with the source and drain electrodes but with different barrier heights of Φ_S and Φ_D, respectively (Fig. 6B-a). When the drain is forward

biased, the quasi-Fermi levels at the source ($E_{F,S}$) and drain ($E_{F,D}$) are different by the value of eV_{bias}, where V_{bias} is the applied bias (Fig. 6B-b). An externally applied mechanical strain (ε_g) results in both band structure change and piezoelectric potential field in a ZnO NW. The former leads to the piezoresistance effect, a red shift in local photoluminescence [31] and an enhanced photocurrent [32], which is a non-polar and symmetric effect at the both source and drain contacts. Since ZnO is a polar structure along *c*-axis, straining in axial direction (*c*-axis) creates a polarization of cations and anions in the NW growth direction, resulting in a piezopotential drop from V^+ to V^- along the NW, which produces an asymmetric effect on the changes in the SB heights (SBHs) at the drain and source electrodes. Under tensile strain, the SBH at the source side reduces from Φ_S to $\Phi'_S \cong \Phi_S - \Delta E_P$ (Fig. 6B-c), where ΔE_P denotes the effect from the locally created piezopotential and it is a function of the strain, resulting in increased I_{DS}. For the compressively strained SGT, the sign of the piezopotential is reversed, thus the SBH at the source side is raised from Φ_S to $\Phi''_S \cong \Phi_S + \Delta E'_P$ (Fig. 6B-d), where $\Delta E'_P$ denotes the piezopotential effect on the SBH at source side, resulting in a large decrease in I_{DS}. Therefore, as the strain ε_g is swept from compressive to tensile regions, the I_{DS} current can be effectively turned from ''on'' to ''off'' while V_{DS} remains constant. This is the fundamental principle of the SGT.

Logic operations of NW strain-gated NAND and NOR gates were realized by integrating SGTs, which are gated individually by the applied strains, according to corresponding layout rules (Fig. 7A-a and A-b for NAND gate and Fig. 7B-a and B-b for NOR gate) [29]. The output voltages of NAND and NOR gates versus the input gate strains are shown in Fig. 7A-c for NAND gate and Fig. 7B-c or NOR gate. Two types of transitions occur during the switching operation of both the ZnO NW strain-gated NAND and NOR gates. It can also be seen that NW strain-gated NAND and NOR gates with active loads (Figs. 7A-c and B-c) exhibit better overall performance, such as larger logic swing, compared to passive-load NAND and NOR gates. Using the SGTs as building blocks, other universal logic components such as inverters and XOR gates have been demonstrated for performing piezotronic logic calculations, which have the potential to be integrated with the current NEMS technology for achieving advanced and complex functional actions in nanorobotics, microfluidics and micro/nano-systems.

Strain sensor

The sensitive response of the transport behavior of ZnO NWs to the external strain has been used for the fabrication of a series of devices. Fig. 5B shows how the strain affects the electric property of the device consisting of a ZnO NW and silver electrodes [22,23]. The device showed a rectification behavior before it was strained. When the device was stretched or compressed, the *I*—*V* behavior changed as well. With the same forward bias, the tensile strain increased the current while the compressive strain decreased the current. Detailed data analysis and simulation can derive the effective change in SB height in corresponding to the applied strain besides the change in conductivity due piezoresistance effect [22,23]. The performance of a strain sensor is characterized by a gauge factor, which is defined to be the slope of the normalized current (*I*)—strain (ε) curve, $[\Delta I(\varepsilon)/I(0)]/\Delta\varepsilon$. The highest gauge factor demonstrated for our sensor device is 1250 although the diameter of the ZnO wire used for the measurement was $\sim$1 μm, which is much higher than the gauge factor of conventional metal strain gauges (1—5) and state-of-the-art doped-Si strain sensor ($\sim$200), and even higher than the highest gauge factor reported for CNTs ($\sim$1000) [33]. It is anticipated that if the measurement is made using NWs, the gauge factor can be improved by orders of magnitude.

Hybrid field-effect-transistor [34]

Single-walled carbon nanotube (SWNT) field effect transistor (FET) is one of the most fundamental nanodevices in one-dimensional nanomaterials, in which the SWNT is connected by two electrodes as current channel, and a third electrode is built on the top/bottom of the SWNT channel as a gate. The carrier transport process in SWNT is modulated by an externally applied gate voltage. We have demonstrated the first ZnO NW and SWNT hybrid FET, in which the piezopotential created by an externally applied strain in a ZnO NW serves as a gate voltage for controlling the carrier transport in a SWNT based current channel located underneath. The ZnO NW serves as an electric-power-free and contact-free gate. This device is a unique coupling between the piezoelectric property of ZnO NW and the semiconductor performance of SWNT with a full utilization of its mobility.

The magnitude of the piezopotential in our hybrid device can be directly quantified by comparing the amount of current change ΔI_{DS} of an FET when it is gated by piezopotential in reference to when it is gated by a top-electrode (see Fig. 8). Since ZnO NWs have both piezoelectric and semiconducting properties, it can possibly be used as a metal gate electrode for FET, even if there is potential drop due to the limited charge carrier in a ZnO wire. At first, we used the ZnO wire as a through path for outside gate voltage. In the measurement, the drain—source voltage bias V_{DS} was fixed at 1 V, while outside gate voltage V_G through the ZnO wire was swept to modulate the drain—source current I_{DS} (red dots in Fig. 8). Afterward, the current change I_{DS} due to the piezopotential (black dot in Fig. 8) was measured by applying an external deformation on the hybrid device but without applying a gate voltage. When the strain of 0.05% was applied along the ZnO wire used for the same device, drain—source current I_{DS} was increased suddenly, which is plotted as a function of time in the same diagram. The piezopotential is directly received by examining the corresponding change in gate voltage of the FET when it was operated in conventional mode in corresponding to the change of ΔI_{DS}, as shown by the dotted line in Fig. 8. The piezopotential for a strain of 0.05% was $\sim$0.65 V. This study shows the feasibility of using piezopotential as gate voltage for another device.

Sensors and triggers using free-standing beam [35]

NW nanodevices are mostly laterally bonded on a flat substrate following the configuration of a FET, in which

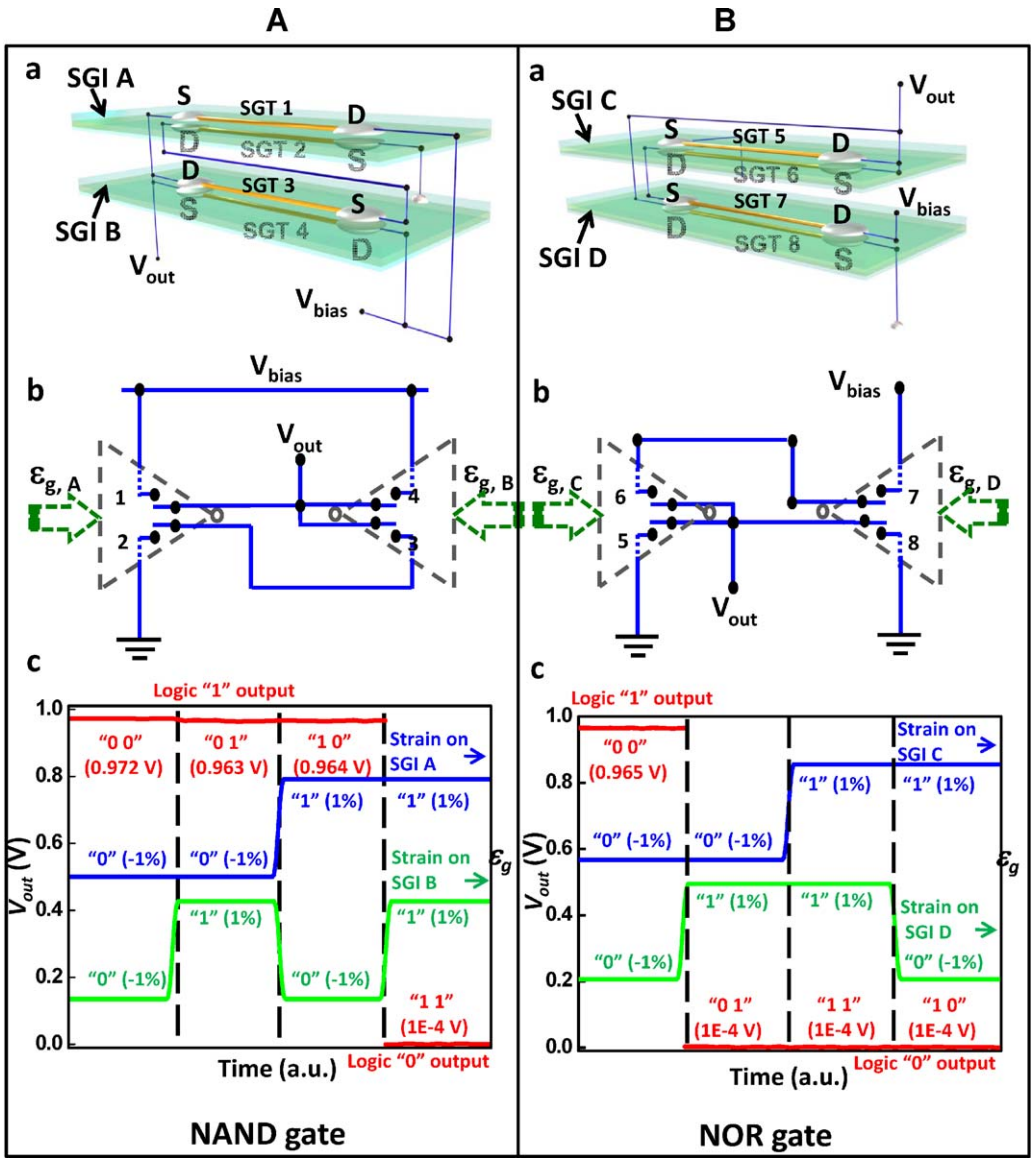

Figure 7 Strain gated piezotronic logic operation. (A) ZnO NW strain-gated NAND gate. (a) Schematic representation of the ZnO NW strain-gated NAND logic gate, which is composed of two strain gated inverter (SGIs), SGI A and SGI B. The strain input A for SGI A is defined in reference to the strain applied to SGT 2 and the strain input B for SGI B is defined in reference to the strain applied to SGT 3. (b) Layout for ZnO NW strain-gated NAND logic gate by connecting two ZnO NW SGIs. (c) Logic operations and experimental truth table of the ZnO NW strain-gated NAND logic gate. Red line is the electrical output of the NAND gate. Blue and green lines represent the strain inputs applied on SGI A and SGI B respectively. ''1'' and ''0'' in the quotation marks along the input curves represent the logic levels of the inputs. For the output, the first number in the quotation marks represents the logic level for strain input on SGI A and the second number represents the logic level for strain input on SGI B. The values in the parenthesis are the corresponding physical values for the inputs and output. The same denominations apply for NOR and XOR logic gates. (B) ZnO NW strain-gated NOR gate. (a) Schematic of the ZnO NW strain-gated NOR logic gate, which is composed of two SGIs, SGI C and SGI D. The strain input C for SGI C is defined in reference to the strain applied to SGT 5 and the strain input D for SGI D is defined in reference to the strain applied to SGT 8. (b) Layout for ZnO NW strain-gated NOR logic gate connecting two ZnO NW SGIs. (c) Logic operations and experimental truth table of the ZnO NW strain-gated NOR logic gate. Red line is the electrical output of the NOR gate. Blue and green lines represent the strain inputs applied on SGI C and SGI D, respectively. (For interpretation of the references to colour in this figure legend, the reader is referred to the web version of the article.)
From [29].

the substrate serves as a gate electrode; the current transported from the drain to source along the NW is controlled or tuned by the applied gate voltage or the chemical/biochemical species adsorbed on the surface of the NWs. We have demonstrated a piezoelectric-potential gated force/vibration sensor using a free standing ZnO wire. In this device, the key functional part is the junction region at the root of the ZnO wire, and the top is a free vibrational end

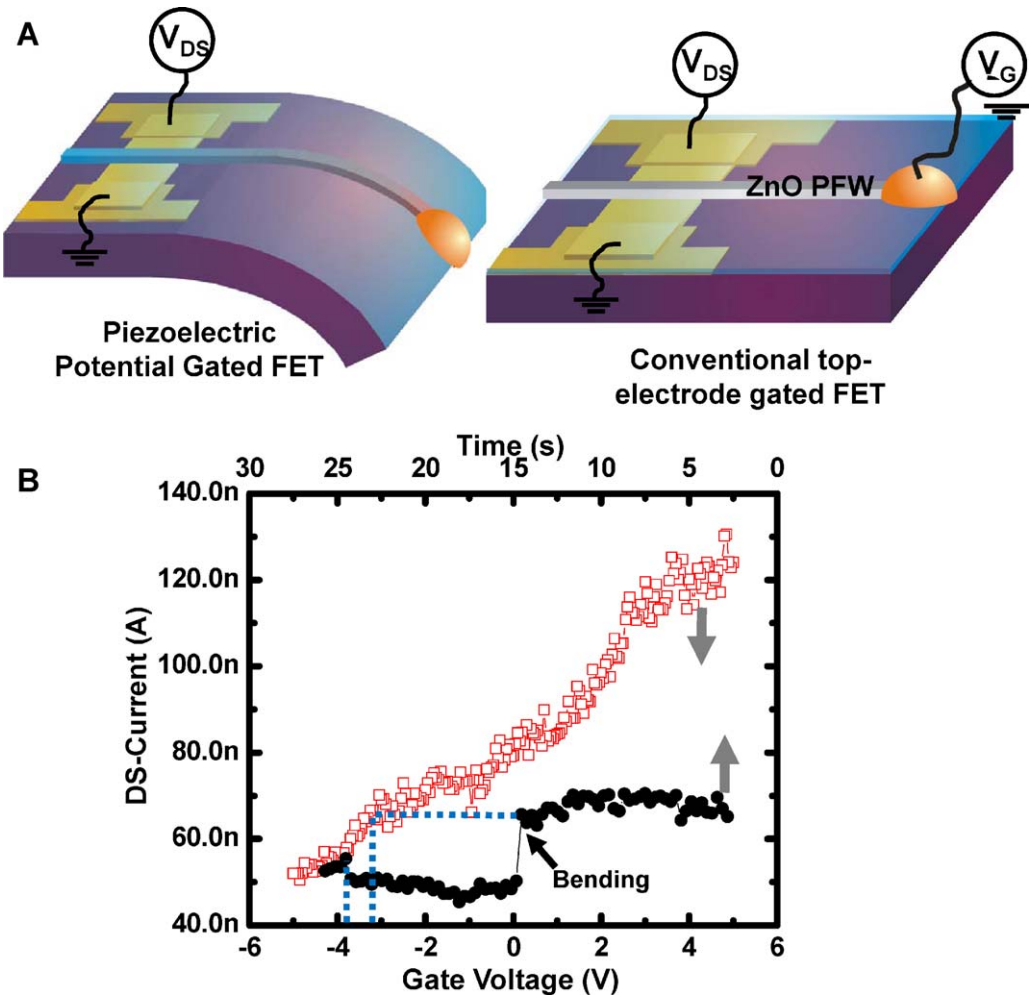

Figure 8 Hybrid FET by using the piezopotential in ZnO as the gate voltage for a SWNT based transistor. (A) Schematics of a carbon nanotube FET when it is gated by a conventional top-electrode through the ZnO wire (left-hand side), and when it is gated by the piezoelectric potential created by the wire by straining (right-hand side). (B) Overlapped plot of a positive transconductance FET when it was operated in top-electrode gated mode by using swiping the gate voltage and when it was gated by piezopotential at a tensile strain of 0.05% (with on and off positions marked) as a function of time.
From [34].

(Fig. 9B). Once subjected to mechanical impact/triggering, the bent ZnO wire cantilever creates a piezoelectric potential distribution across its width in the root/junction region, and simultaneously produces local depletion and reverse depletion layers (Fig. 9A) [36]. The size of the area and the local donor concentration of the reverse depletion layer are both dominated by the external force/pressure/vibration induced piezoelectric potential. By periodically blowing a gentle airflow onto the wire device, the current flowing through the device changed drastically (Fig. 9C). This work presents a new approach towards nanosensors that utilizes the self-generated piezoelectric-potential to control the transverse performance of the device. The sensor device has been proved to have a high piezoelectric-potential control sensitivity ($\sim$2%/μN) in micron scale due to the free standing cantilever structure and fairly stable linear relationship between the mechanical stimulation and its electrical response. At the same time, it has a response time less than 20 ms. The device has potential applications as hearing aids, AFM cantilevers, force/pressure sensors, and security systems.

Piezo-phototronic devices and applications

As demonstrated in Fig. 2, strain can effectively increase the height of the SB in ZnO wire, allowing a fine tuning of the electric transport property of the device. In contrast, the effective height of the SB can be lowered by shining a laser beam at the local contact with excitation energy larger than the bandgap, which increases the density of the local electron—hole pairs and the change of barrier profile due to charge separation/redistribution. By controlling the magnitude of the strain and the intensity of the laser beam, we can effectively tune the charge transport property from Schottky to Ohmic or from Ohmic to Schottky by controlling the SB height. Our study shows that the Schottky contacted UV detector has a much higher sensitivity and responsivity

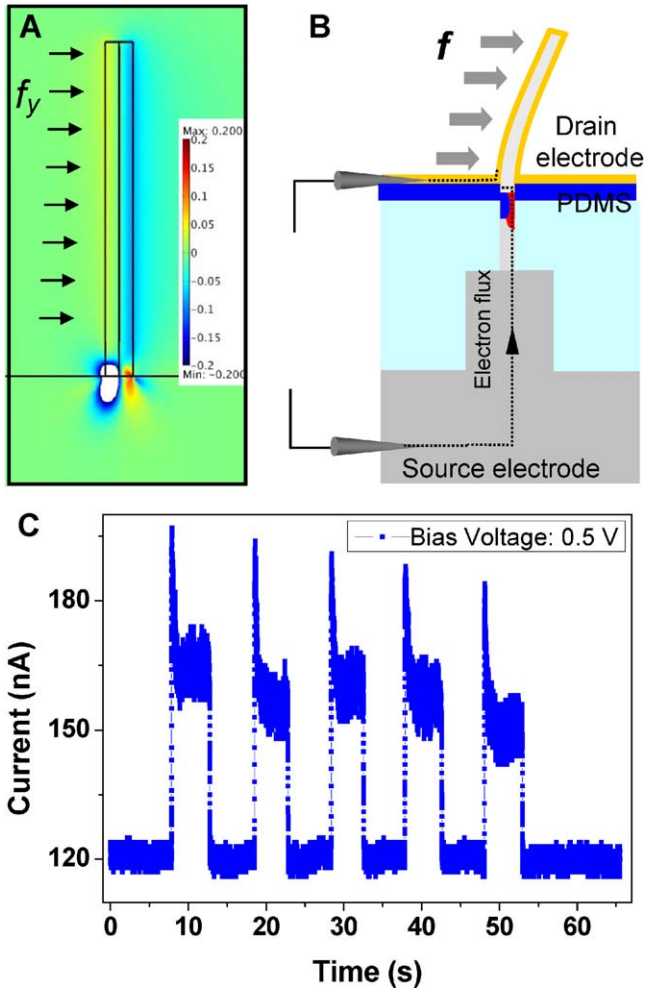

Figure 9 Piezopotential gated transistor as force/vibration sensor. (A) Plot of piezoelectric potential distribution φ for a donor concentration $n = 1 \times 10^{23}$ m^{-3} after considering screening effect by free charge carriers using a static model. A schematic diagram of the vertical wire is shown at the left. The dimension of the wire is width $d = 25$ nm, length $l = 600$ nm. There is a potential region at the junction of the ZnO wire and ZnO substrate, which shows a reverse potential distribution comparing to the upper part of the wire with positive potential at the compressive side and negative potential at the tensile side. The blank region is the region where $\varphi \ll -0.2$ V. (B) A design of free standing ZnO wire cantilever sensor device. In this device, free standing cantilever makes it easily to response to a tiny external force and then show piezoelectric effect. At the same time, in its working status, the free charge carriers are guaranteed to flow through the junction region between the cantilever part and on-substrate part to make sure the force induced variation of electrical property can be detected by the measurement system. (C) Response of a device to a periodic gas blowing for demonstrating its potential application for measuring the transverse force/pressure. The current transported by the device at a fixed bias of 0.5 V when Argon gas was blown at the wire as short pulses.
From [35].

as well as recover time than the Ohmic contacted nanowire devices [37].

To illustrate the piezo-phototronic effect, we have fabricated a two-end bonded ZnO wire device. Owing to the variation in local contacts, the device shows an asymmetric I—V transport property. Both piezoelectric effect and photoexcitation intensity can tune the I—V transport property of a ZnO microwire device, but they act in opposite directions. If we refer one end of the device as A, by shining the laser at contact A of the device, as the relative intensity of the light being changed via optical filters from transmission coefficient $T = 0.001$ to 1, the I—V curve has been largely tuned (Fig. 9A). Fine tuning of the magnitude of mechanical straining and the intensity of the light illumination can produce a designed shape of the I—V characteristic. Fig. 9B shows the coupled tuning of the two effects on the I—V shape. By choosing a strain of −0.2% and relative light intensity $T = 0.01$ (green curve), the observed I—V curve matched well to the original I—V curve obtained without applying a strain nor laser excitation (dark curve). This experiment shows the possibility of controlling the I—V characteristic of a NW device by piezo-phototronic effect [11]. We now present a few applications of the piezo-phototronic effect.

Maximizing photocell power output [38]

By exciting a SB structure using a laser that has photon energy higher than the bandgap of the semiconductor, electron—hole (e—h) pairs are generated at the interface region. If the height of the SB is too high, the generated e—h pairs cannot be effectively separated, resulting in no photon induced current. If the SB is too low, the e—h pairs are easily recombined even after a short separation, again there is no photon current. There exists an optimum SB height that gives the maximum output photon current. By using the tuning effect of piezopotential to the SB, we can experimentally find out the optimum choice of SB height in corresponding to the maximum photon current.

We now use the M—S—M contacted microwire to illustrate the effect of the piezopotential on the performance of a photocell. First, by shining a laser of wavelength 325 nm, the output current was recorded from the device when the laser spot was focused at different positions on the device, as shown in Fig. 10A. The entire device is constructed with two back-to-back SBs connected via the microwire. When the focal point of the laser beam was changed from one SB to the other, the measured output current also changed its sign. This is due to the opposite directions of the local electrical fields at the two SB areas, which enforce the separation of electrons and holes induced by the laser irradiation, and thus lead them to flow in opposite directions. If we fixed the laser beam at one SB area, and bend the substrate of the device step by step, strain will be introduced into the device step by step. This will alter the effective heights of the two SBs and thus the characteristic of the microwire photocell.

Fig. 10B shows the measured photon current of a device as a function of the applied strain. It is apparent that the output reached a maximum at a tensile strain of 0.12%. This is an example of using piezoelectric effect to enhance

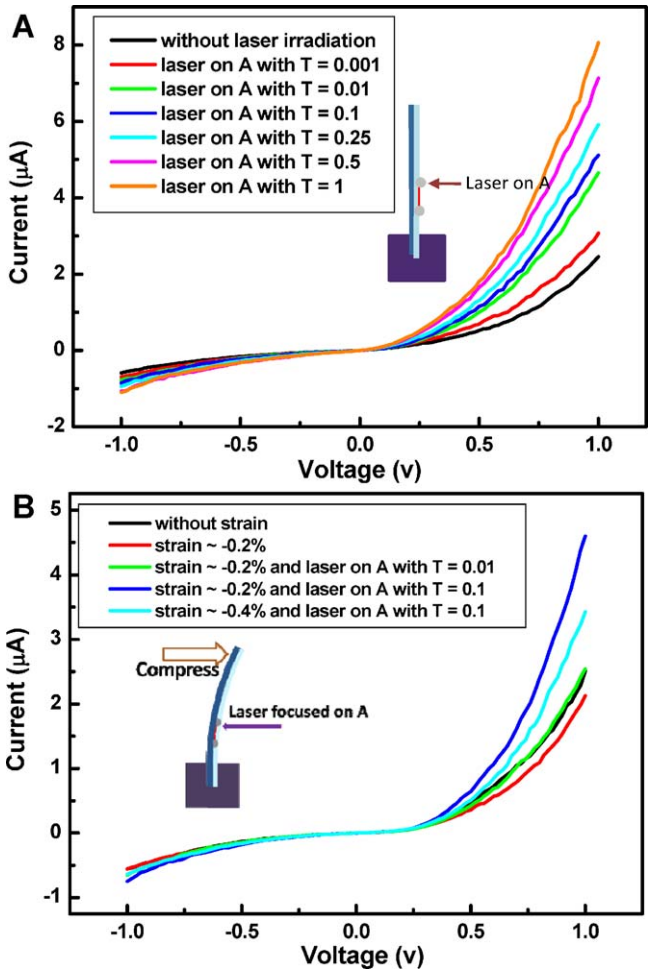

Figure 10 Piezo-phototronic effect by coupling among piezoelectric, photon excitation and semiconductor properties. (A) Tuning the *I*—*V* transport characteristic of a device by controlling the intensity of the excitation laser focused at contact A via optical filters from transmission coefficient $T = 0.001$ to 1, without strain. (B) Design and control of the transport properties of the device by coupling the intensity of illuminating laser and the degree of straining in the microwire showing the basic principle of piezo-phototronics. The insets are the corresponding configuration of the two-end bonded nanowire device.
From [11].

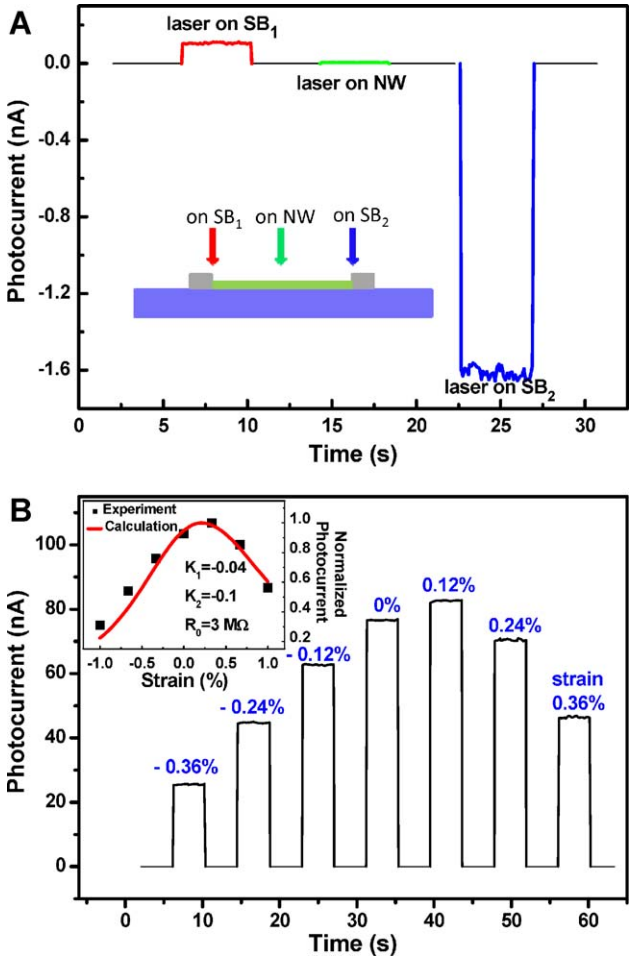

Figure 11 Maximizing the photocell output by piezo-phototronic effect. (A) Measured output current when the laser spot was focused at different positions of the wire. The inset shows the sketched picture to indicate the related illuminating position of the laser on the device. (B) Output current responses to the strain applied on a device. The inset is the simulated result based on an equivalent circuit model.
From [38].

the photon-electron generation process by using the piezo-phototronic effect. Such a study is beneficial for solar cell research for maximizing the output power by introducing strain during the device fabrication.

Enhancing photon detection sensitivity [39]

The basic principle of a photon detector is based on photoelectric effect, in which the e-h pairs generated by a photon are separated by either a pn junction or a SB. In such a case, the height of the SB, for example, is important for the detection sensitivity of the photon detector (Fig. 11). By tuning the SB height in a ZnO wire based UV sensor through applying a strain, we may improve the sensitivity of the UV detector especially when the illumination intensity is rather weak. Our experimental set up is presented in Fig. 12A, which is an integration of strain stage, a laser excitation source and the electrical measurement system of the device. The responsivity of the photodetector is respectively enhanced by 530%, 190%, 9% and 15% upon 4.1 pW, 120.0 pW, 4.1 nW, 180.4 nW UV light illumination onto the wire by introducing a −0.36% compressive strain in the wire (Fig. 12B), which effectively tuned the SB height at the contact by the produced local piezopotential. The sensitivity for weak light illumination is especially enhanced by introducing strain, although the strain almost has little effect on the sensitivity to stronger light illumination. Our results show that the piezo-phototronic effect can enhance the detection sensitivity more than fivefold for pW levels light detection.

Nanowires rather than thin films, why?

The principles illustrated for piezotronics and piezo-phototronics apply to both of thin film and NWs. But the

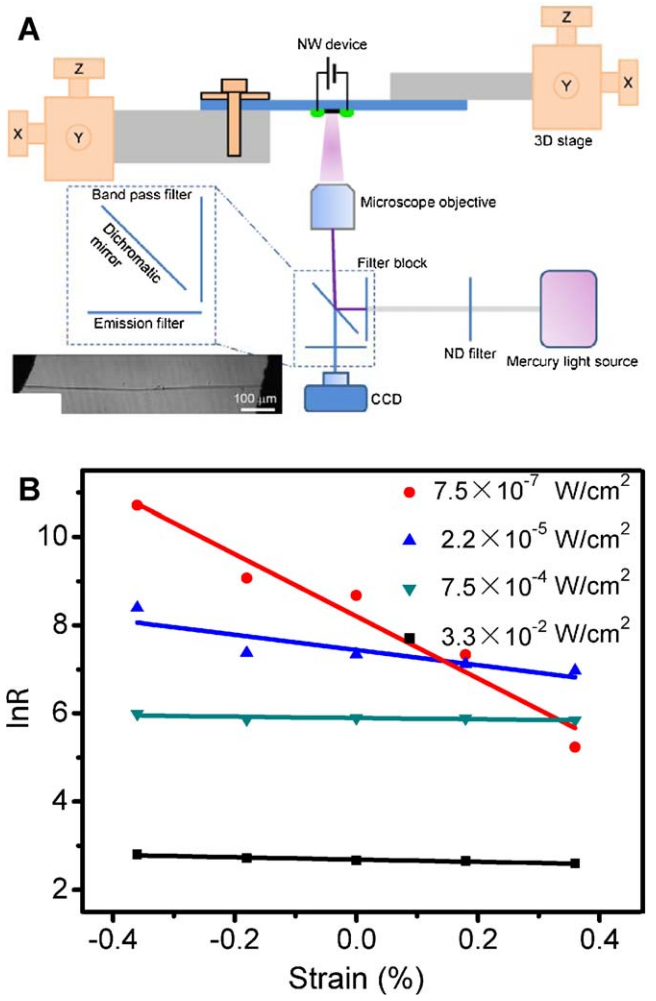

Figure 12 Enhancing photon detection sensitivity by piezo-phototronic effect. (A) Schematic diagram of the measurement system to characterize the performance of the piezopotential tuned photodetector. An optical microscopy image of a ZnO wire device is shown. (B) Responsivity of a ZnO wire UV detector (in units of A/W) as a function of strain under different excitation light intensities on a natural logarithmic scale.
From [39].

NWs are of great advantageous than thin films for the following reasons. First, ZnO NWs can be grown using chemical approach at low temperature (<100 °C) on any substrate and any shape substrate, exhibiting a huge advantage for scaling up at a low cost [3]; while it is practically difficult to make high quality single crystal thin film at low temperature. Secondly, owing to the largely reduced size, NWs exhibit extremely high elasticity that allows large degrees of mechanical deformation (up to 6% in tensile strain according to theoretical calculation for very small wire [40]) without cracking or fracture, while thin film can easily generate cracks after applying even smaller strain. Third, the small size of the NWs largely increases the toughness and robustness of the structure so that it is almost fatigue free. Fourth, a relatively small force is required to induce the mechanical agitation, so that it can be very beneficial for building ultrasensitive devices. Finally, NWs may exhibit higher piezoelectric coefficient than thin film [41].

Although the examples illustrated in this article were made using wires with diameter from 200 to 1000 nm and lengths up to 300 μm for the purpose of easy manipulation and the demonstration of the proposed effect, once these designs can be fabricated using NWs with diameter of 10—30 nm, the performance of the device is expected to improve by orders of magnitude. The principle and design demonstrated here are general and can be applied to a range of size of structures.

Summary and outlook

Piezopotential is created in a piezoelectric material by applying a stress, and it is generated by the polarization of ions in the crystal. The introduction of this inner potential in semiconductor materials can significantly change/modify the band structure at a pn junction or metal—semiconductor Schottky barrier, resulting in significant change in the charge transport property. This is the core science of piezoelectricity on electronic and photonic devices.

Piezotronics is about the electronics fabricated by using piezopotential as a ''gate'' voltage for controlling the charge transport process. Its applications have been demonstrated as diode, strain/force/sensors, triggers, and logic gates.

Piezo-phototronics is a result of three-way coupling among piezoelectricity, photonic excitation and semiconductor transport. This effect allows tuning and controlling of electro-optical process by strain induced piezoelectric potential, with potential applications in light emitting diode, photocell and solar cell, and photon detector.

Although the response time of the piezotronics is slower than the conventional CMOS technology and it is mostly likely to work at lower frequencies, the functionality it offers are complimentary to CMOS technology. An effective integration of piezotronic and piezo-phototronic devices with silicon based CMOS technology, unique applications can be found in areas such as human—computer interfacing, sensing and actuating in nanorobotics, smart and personalized electronic signatures, smart MEMS/NEMS.

Acknowledgements

Thanks to the support from DARPA, BES DOE, NSF, Airforce, KAUST and WPI (NIMS). Thanks to Xudong Wang, Jr-Hau He, Jun Zhou, Yaguang Wei, Wenzhuo Wu, Youfan Hu, Yan Zhang, Qing Yang, Yifan Gao, Weihua Liu, Minbaek Lee, Peng Fei, and other members and collaborators for their contributions.

References

[1] Z.L. Wang, J.H. Song, Science 312 (2006) 242—246.
[2] Z.L. Wang, Adv. Funct. Mater. 18 (2008) 3553—3567.
[3] Z.L. Wang, Mater. Sci. Eng. R 64 (2009) 33—71.
[4] Z.L. Wang, R.S. Yang, J. Zhou, Y. Qin, C. Xu, Y.F. Hu, S. Xu, Mater. Sci. Eng. R (2010), doi:10.1016/j.mser.2010.06.015.
[5] Z.L. Wang, Adv. Mater. 19 (2007) 889—992.
[6] Z.L. Wang, J. Phys. Chem. Lett. 1 (2010) 1388—1393.
[7] S.J. Tans, A.R.M. Verschueren, C. Dekker, Nature 393 (1998) 49—52.

[8] T. Rueckes, K. Kim, E. Joselevich, G.Y. Tseng, C.L. Cheung, C.M. Lieber, Science 289 (2000) 94—97.
[9] X.D. Wang, J. Zhou, J.H. Song, J. Liu, N.S. Xu, Z.L. Wang, Nano Lett. 6 (2006) 2768—2772.
[10] J.H. He, C.L. Hsin, J. Liu, L.J. Chen, Z.L. Wang, Adv. Mater. 19 (2007) 781—784.
[11] Y.F. Hu, Y.L. Chang, P. Fei, R.L. Snyder, Z.L. Wang, ACS Nano 4 (2010) 1234—1240.
[12] Y.F. Gao, Z.L. Wang, Nano Lett. 7 (2007) 2499—2505.
[13] Z.Y. Gao, J. Zhou, Y.D. Gu, P. Fei, Y. Hao, G. Bao, Z.L. Wang, J. Appl. Phys. 105 (2009) 113707.
[14] X.D. Wang, J.H. Song, J. Liu, Z.L. Wang, Science 316 (2007) 102—105.
[15] Y. Qin, X.D. Wang, Z.L. Wang, Nature 451 (2008) 809—813.
[16] R.S. Yang, Y. Qin, L.M. Dai, Z.L. Wang, Nat. Nanotechnol. 4 (2009) 34—39.
[17] S. Xu, Y. Qin, C. Xu, Y.G. Wei, R.S. Yang, Z.L. Wang, Nat. Nanotechnol. 5 (2010) 366—373.
[18] G. Zhu, R.S. Yang, S.H. Wang, Z.L. Wang, Nano Lett. 10 (2010) 3151—3155.
[19] S. Xu, B.J. Hansen, Z.L. Wang, Nat. Commun., doi:10.1038/ncomms1098.
[20] Y.F. Hu, Y. Zhang, C. Xu, G. Zhu, Z.L. Wang, Nano Lett., doi:10.1021/nl103203u.
[21] Z.T. Li, Z.L. Wang, Adv. Mater, online.
[22] J. Zhou, Y.D. Gu, P. Fei, W.J. Mai, Y.F. Gao, R.S. Yang, G. Bao, Z.L. Wang, Nano Lett. 8 (2008) 3035—3040.
[23] J. Zhou, P. Fei, Y.D. Gu, W.J. Mai, Y.F. Gao, R.S. Yang, G. Bao, Z.L. Wang, Nano Lett. 8 (2008) 3973—3977.
[24] S.S. Kwon, W.K. Hong, G. Jo, J. Maeng, T.W. Kim, S. Song, T. Lee, Adv. Mater. 20 (2008) 4557—4562.
[25] D.A. Scrymgeour, J.W.P. Hsu, Nano Lett. 8 (2008) 2204—2209.
[26] Y. Yang, J.J. Qi, Q.L. Liao, H.F. Li, Y.S. Wang, L.D. Tang, Y. Zhang, Nanotechnology 20 (2009) 125201.
[27] A. Asthana, K. Momeni, A. Prasad, Y.K. Yap, R.S. Yassar, Appl. Phys. Lett. 95 (2009) 172106.
[28] K.H. Liu, P. Gao, Z. Xu, X.D. Bai, E.G. Wang, Appl. Phys. Lett. 92 (2008) 213105.
[29] W.Z. Wu, Y.G. Wei, Z.L. Wang, Adv. Mater. (2010), doi:10.1002/adma.201001925.
[30] T. Thorsen, S.J. Maerkl, S.R. Quake, Science 298 (2002) 580—584.
[31] X.B. Han, L.Z. Kou, X.L. Lang, J.B. Cia, N. Wang, R. Qin, J. Lu, J. Xu, Z.M. Liao, X.Z. Zhang, X.D. Shan, X.F. Song, J.Y. Gao, W.L. Guo, D.P. Yu, Adv. Mater. 21 (2009) 4937—4942.
[32] P. Gao, Z.Z. Wang, K.H. Liu, Z. Xu, W.L. Wang, X.D. Bai, E.G. Wang, J. Mater. Chem. 19 (2009) 1002—1005.
[33] J. Cao, Q. Wang, H.J. Dai, Phys. Rev. Lett. 90 (2003) 157601.
[34] W.H. Liu, M. Lee, L. Ding, J. Liu, Z.L. Wang, Nano Lett. 10 (2010) 3084—3089.
[35] P. Fei, P.H. Yeh, J. Zhou, S. Xu, Y.F. Gao, J.H. Song, Y.D. Gu, Y.Y. Huang, Z.L. Wang, Nano Lett. 9 (2009) 3435—3439.
[36] Y.F. Gao, Z.L. Wang, Nano Lett. 9 (2009) 1103—1110.
[37] J. Zhou, Y.D. Gu, Y.F. Hu, W.J. Mai, P.H. Yeh, G. Bao, A.K. Sood, D.L. Polla, Z.L. Wang, Appl. Phys. Lett. 94 (2009) 191103.
[38] Y.F. Hu, Y. Zhang, Y.L. Chang, R.L. Snyder, Z.L. Wang, ACS Nano 4 (2010) 4220—4224.
[39] Q. Yang, X. Guo, W.H. Wang, Y. Zhang, S. Xu, D.H. Lien, Z.L. Wang, ACS Nano 4 (2010) 6285—6291.
[40] R. Agrawal, B. Peng, H.D. Espinosa, Nano Lett. 9 (2009) 4177—4183.
[41] M.H. Zhao, Z.L. Wang, S.X. Mao, Nano Lett. 4 (2004) 587—590.

Dr. **Zhong Lin Wang** is the Hightower Chair in Materials Science and Engineering, Regents' professor, Engineering distinguished professor and director, Center for Nanostructure Characterization, at Georgia Tech. Dr. Wang is a foreign member of the Chinese Academy of Sciences, member of European Academy of Sciences, fellow of American Physical Society, fellow of AAAS, fellow of Microscopy Society of America and fellow of Materials Research Society. He has received the 2001 S.T. Li prize for Outstanding Contribution in Nanoscience and Nanotechnology, the 1999 Burton Medal from Microscopy Society of America, and the 2009 Purdy award from American Ceramic Society. Dr. Wang has made original and profound contributions to the synthesis, discovery, characterization and understanding of fundamental physical properties of oxide nanobelts and nanowires, as well as applications of nanowires in energy sciences, electronics, optoelectronics and biological science. He invented and pioneered the *in situ* technique for measuring the mechanical and electrical properties of a single nanotube/nanowire inside a transmission electron microscope (TEM). His breakthroughs in developing nanogenerators establish the principle and technological road map for harvesting mechanical energy from environment and biological systems for powering a personal electronics. He initiated, coined and pioneered the field of piezotronics and piezo-phototronics by introducing piezoelectric potential gated charge transport process in fabricating new electronic and optoelectronic devices, which have potential applications in MEMS/NEMS, nanorobotics, human—electronics interface, sensors, medical diagnosis and photovoltaic. Dr. Wang is the world's top 5 most cited authors in nanotechnology and materials science. He has published four scientific reference and textbooks and over 640 peer reviewed journal articles, 45 book chapters, edited and co-edited 14 volumes of books on nanotechnology, and held 28 patents. His entire publications have been cited for over 38,000 times. The H-index of his citations is 92. Details can be found at: http://www.nanoscience.gatech.edu/zlwang.